Structural Changes Due to the Deprotonation of the Proton Release Group in the M Photointermediate of Bacteriorhodopsin as Revealed by Time-Resolved FTIR Spectroscopy

Joel E. Morgan[1], **Ahmet S. Vakkasoglu**[2], **Johan Lugtenburg**[3], **Robert B. Gennis**[2,4], and **Akio Maeda**[4,*]

[1]Department of Biology, Center for Biotechnology and Interdisciplinary Studies, Room 2137, Rensselaer Polytechnic Institute, 110 Eighth St., Troy, NY 12180 [2]Center for Biophysics and Computational Biology, University of Illinois at Urbana-Champaign, Urbana, IL, 61801 [3]Chemistry Department, Gorlaus Laboratories, Leiden University, Leiden, The Netherlands [4]Department of Biochemistry, University of Illinois at Urbana-Champaign, Urbana, IL 61801

Abstract

One of the steps in the proton pumping cycle of bacteriorhodopsin (BR) is the release of a proton from the proton-release group (PRG) on the extracellular side of the Schiff base. This proton release takes place shortly after deprotonation of the Schiff base (L-to-M transition), and results in an increase in the pK_a of Asp85, which is a crucial mechanistic step for one-way proton transfer for the entire photocycle. Deprotonation of the PRG can also be brought about without photoactivation, by raising the pH of the enzyme (pK_a of PRG; ~9). Thus comparison of the FTIR difference spectrum for formation of the M intermediate (M minus initial unphotolyzed BR state) at pH 7 to the corresponding spectrum generated at pH 10 may reveal structural changes specifically associated with deprotonation of the PRG. Vibrational bands of BR that change upon M formation are distributed across a broad region between 2120 and 1685 cm^{-1}. This broad band is made up of two parts. The band above 1780 cm^{-1}, which is insensitive to C_{15}-deuteration of the retinal, may be due to a proton delocalized in the PRG. The band between 1725 and 1685 cm^{-1}, on the lower frequency side of the broad band, is sensitive to C_{15}-deuteration. This band may arise from transition dipole coupling of the vibrations of backbone carbonyl groups in helix G with the side chain of Tyr57 and with the C_{15}—H of the Schiff base. In M these broad bands are abolished, and the 3657 cm^{-1} band, which is due to the disruption of the hydrogen bonding of a water molecule, probably with Arg82, appears. Loss of the interaction of the backbone carbonyl groups in helix G with Tyr57 and the Schiff base, and separation of Tyr57 from Arg82, may be causes of these spectral changes, leading to the stabilization of the protonated Asp85 in M.

Bacteriorhodopsin from *Halobacterium salinarum,* a light-driven proton pump, is a fascinating integral membrane protein that is well suited for the study of protein function in terms of structural dynamics. Light energy that is absorbed by the all-*trans* retinal cofactor, linked to Lys216 through the protonated Schiff base, causes *trans*-to-*cis* isomerization of the $C_{13}=C_{14}$ bond of the retinal. Spectroscopic studies have revealed a series of intermediates, known as K, L, M, N, and O (1, 2), which appear on time scales from picoseconds to milliseconds after initiation of the photocycle by a flash. Individual proton transfer steps between internal residues occur during the transitions between intermediates, resulting in the net transport of one proton across the membrane. FTIR spectroscopic studies on the

---

[*]To whom correspondence should be addressed. Telephone and Fax: +81-774-22- 8781. akio.maeda@gmail.com.

photocycle, using mutants, have revealed a great deal about the role of individual amino acid residues and internal water molecules in these proton transfer steps.

The L-to-M transition in the photocycle is the first step of the mechanism in which proton transfer takes place, with the movement of a proton from the Schiff base, near the center of the membrane, to Asp85 on the extracellular side. FTIR studies at low temperatures have shown that the L-to-M transition is accompanied by several structural changes, one of which is the relocation of a water-containing cavity on the cytoplasmic side, from a location close to the Schiff base, to a more distant site near Asp96-Phe219, about 1 nm from the Schiff base (reviewed in 3, 4). Previous microsecond time-resolved FTIR spectroscopic studies by Morgan et al (5) have revealed that there is a less rigid structure of internal water molecules characteristic of L at room temperature. A subsequent study by Lórenz-Fonfría et al. (6), however, failed to detect such internal water molecules. This discrepancy could arise from the fact that the FTIR spectroscopy in Lórenz-Fonfría et al. (6) was carried out using bacteriorhodopsin films with low hydration (93% humidity), which apparently led to the loss of the vibrations due to the internal water of L, as revealed by mono-exponential decay of the intensity of water vibrations and smaller (about half) intensity of the water vibrations in the spectrum of L in comparison to those obtained with the highly hydrated films used by Morgan et al (5). It is known that, with decreasing hydration, the efficiency of proton transfer, as revealed by photoelectric signals, decreases, with an accompanying increase in the population that returns directly from M to initial unphotolyzed state of bacteriorhodopsin (7, 8). These results suggest that internal water molecules, characteristic of L, play a role in the mechanism of proton pumping.

Formation of M is also followed by proton release to the extracellular medium from a site close to the surface (9). This site is referred to as the proton-release group (PRG) (10). Studies of the proton release step using mutants have shown that the residues Glu204 (11), Glu194 (12, 13), Tyr83 (14), Arg82 (15, 16), and Tyr57 (17) are involved in the PRG. Crystallographic studies (18, 19) show that these residues form a hydrogen bonding network together with internal water molecules which they surround. Theoretical studies have proposed that protons release takes place from a protonated water cluster (20, 21). This proton release is proposed to cause the increase in the proton affinity of Asp85 through electrostatic interaction between the PRG and Asp85 (15, 22, 23). The one-way proton transfer may be established in the M state (24), where Asp85 acquires a high proton affinity that does not allow reverse flow of the proton to the Schiff base in the subsequent M-to-N transition. Morgan et al (4) have proposed that this change in proton affinity is driven by the rearrangement of the interactions of Asp212 with Arg82, Tyr57 and water molecules around Asp85. FTIR spectroscopy was applied to investigate this proposal.

Time-resolved FTIR difference spectra of photo-intermediates, referenced to the pre-photolysis state, which has the all-trans retinal, have shown a broad unstructured negative feature in the 2200-1800 cm^{-1} region (6, 25–27). Appearance of this band in the difference spectrum occurs in parallel with the formation of M. The change is abolished when Glu204, a component of the PRG, is mutated to glutamine (E204Q). In this mutant, formation of M is not accompanied by deprotonation of the PRG (22). This suggests a close correlation between the change in the broad band and proton release from the PRG. The broad negative feature becomes more intense as the frequency drops from 2200 cm^{-1} to 1800 cm^{-1}, indicating that the feature extends below 1800 cm^{-1}, where it overlaps with the more intense vibrational bands of the protein and the chromophore.

Alkaline titration of the unphotolyzed bacteriorhodopsin with all-trans retinal chromophore (BR) reveals a transition with a pK_a of ~9, which is closely linked to the protonation state of Asp85 (15). The transition at this pK_a is also responsible for a slight red shift in the visible

spectrum (~1.5 nm) in the initial unphotolyzed BR state, and rapid formation of M in the photocycle (28). This rapid formation of M above this "alkaline transition" can be ascribed to the fact that the PRG is already deprotonated before M formation (15, 16). Thus, comparison of the M-minus-BR spectrum generated at pH 10 with that at pH 7 can reveal structural changes specifically associated with the deprotonation of the PRG. Another event in the L-to-M transition is deprotonation of the Schiff base. Vibrations involving interactions with the Schiff base can be explored by using bacteriorhodopsin in which the Schiff base is labeled by deuterium at the C_{15}-position (C_{15}-deuterated bacteriorhodopsin).

In the present study, microsecond time-resolved FTIR spectroscopy was applied to study the photocycle of bacteriorhodopsin at pH 10, and of C_{15}-deuterated bacteriorhodopsin, using highly hydrated films of purple membrane, as in our earlier work (5), in order to reveal the effects of the deprotonation of the PRG and of changes in the interaction with the Schiff base that occur in the L-to-M transition.

MATERIALS AND METHODS

Sample Preparation

Samples of bacteriorhodopsin in the purple membrane, for FTIR spectroscopy, were made by the procedure reported previously (5): Samples at pH 10 were made by first suspending purple membranes in 1.4 ml of 0.1 M carbonate buffer (pH 10), centrifuging, resuspending in water, centrifuging again, and again resuspending in water. To a 100 µL aliquot of bacteriorhodopsin, carbonate buffer (2 µL of 0.1 M, pH 10.0) was added, and the sample was applied to the center of a 25 mm diameter BaF_2 window. Bacteriorhodopsin with C_{15}-deuterated retinal (C_{15}-deuterated bacteriorhodopsin) has been described previously (29). The dried films showed 0.8 to 1.0 absorbance unit at 1658 cm^{-1}. The films were re-hydrated with 0.5 µL of water. The sample cell was sealed and installed in the spectrophotometer as described previously (5).

Data Acquisition and Processing

FTIR data acquisition and analysis were carried out as described previously (5): Measurements were made using a Varian FTS-6000 spectrophotometer in step-scan mode. The results were first analyzed using the global exponential fitting program SplMod (30, see also http://www.s-provencher.com). The data between 2500 and 900 cm^{-1} were used for the fitting. The same fitting procedures were applied to the previously used data sets from unlabeled bacteriorhodopsin at pH 7 in H_2O. The rate constants obtained from SplMod were used to calculate the component spectra $d_i(v)$ across all frequencies in the full data set using a Gaussian elimination method (the mldivide "backslash" function of MATLAB [The MathWorks, Natick, MA]). The output of these fitting procedures, rate constants and spectra, were processed by the method of Chizhov et al. (31) to calculate the results in terms of a linear sequence of irreversible steps. These results were then used to calculate a difference spectrum with respect to the BR state for each intermediate in a linear irreversible kinetic model. For the details, see Morgan et al (5). It is important to emphasize that these are formal intermediates in a kinetic model, which do not have a simple correspondence to the canonical intermediates of the BR photocycle. In the current paper we use the term d-spectra (d_1, d_2, d_3, d_4 and so on with the rate constants of k_1, k_2, k_3, k_4 and so on, respectively, where d_1 is formed at the rate k_1 and decays at k_2) in place of the term b-spectra, used in the previous paper. Spectrum d_0 corresponds to the spectrum of the species immediately after flash, within our time resolution (5 µs). We have changed the nomenclature to avoid possible confusion with the term b-spectra which is commonly used with a different meaning (32).

RESULTS

Spectra of Bactriorhodopsin at pH 10

The entire time-resolved data set at pH 10 (the average of 24 files) was fitted with a six exponential model. The rate constants of 8.3, 1.9, and $0.56*10^3$/sec for k_3, k_4 and k_5, respectively are nearly identical to the corresponding values at pH 7 (7.8, 1.9 and $0.66*10^3$/sec) (5). The higher value of k_2 ($39*10^3$/sec) compared to the corresponding rate constant at pH 7 ($23*10^3$/sec) reflects rapid formation of M at alkaline pH, and the smaller value of k_6 ($0.025*10^3$/sec vs $0.16*10^3$/sec) is due to slower completion of the photocycle at pH 10. It should be noted that the time-constants obtained with rehydrated films of purple membrane at pH 7 are nearly the same as those in solution (31).

Spectrum d_3 in the 1900-900 cm^{-1} region from the pH 10 data (thick line in Figure 1b) shows that the 1184 cm^{-1} band is well below the baseline, indicating nearly complete absence of the spectral components of L and N. This spectrum is nearly coincident in shape with the corresponding spectrum d_3 at pH 7 (Figure 1a, also duplicated by thin lines in Figure 1b), which was assigned to the M-minus-BR spectrum (5). The spectra were normalized by matching their amplitudes at 1200 cm^{-1}. The lifetime of 0.52 ms is also coincident.

Balashov et al (28) have demonstrated two species in the alkaline transition; one is a slightly red-shifted species due to the deprotonation of the PRG (pK_a ~9) and the other, known as P_{480}, is prominent above pH 10. The C=C stretching band at 1528 cm^{-1} of the M-minus-BR spectrum of bacteriorhodopsin at pH 10 (Figure 1b) is almost unchanged from its appearance in bacteriorhodopsin at pH 7, indicating that at pH 10 the photoreaction occurs only in the slightly red-shifted species, which should have a C=C stretching vibration band close to 1528 cm^{-1}, in contrast to P_{480}, in which this band would be expected to have shifted to a distinctly higher frequency.

Even though the spectra at pH 7 and pH 10 are almost completely coincident, there are some differences. A broad negative feature between 1115 and 1035 cm^{-1} that is present in the spectrum at pH 7 is clearly absent at pH 10 (thick versus thin lines in Figure 1b). Within the 2200-1600 cm^{-1} region, more negative intensity is seen in the M-minus-BR spectrum at pH 7 than in that at pH 10. These spectra are compared in Figure 2, with the region from 2200 to 1780 cm^{-1} expanded in the inset; the trace for pH 7 (thin line) clearly tracks below the trace for pH 10 (thick line), beyond the level of noise, throughout the frequency region from 2120 to 1655 cm^{-1} where the two traces merge, though no remarkable structural feature was observed above 1780 cm^{-1}. Spectral changes of this nature have not been noted in previous time-resolved studies at alkaline pH (33–35).

The proton release upon M formation is likely to be abolished or significantly diminished in BR at pH 10 where the alkaline transition due to the titration of the PRG (pK_a = ~9) (10, 15) has already caused deprotonation of the PRG in the BR state. Thus the M-minus-BR spectrum at pH 10 can be used as a reference to subtract contributions that do not arise from the deprotonation of the PRG. In previous work, the contribution of this deprotonation to the FTIR spectrum was assessed by comparing the spectrum obtained from wild-type enzyme, in the 2200-1800 cm^{-1} region, 1 ms after the flash, to the corresponding spectrum of the E204Q mutant (26), in which proton release from the PRG does not occur during the L-to-M transition (11). This difference is similar to the difference between our spectrum d_4 at pH 10, and the corresponding spectrum at pH 7 (d_4, spectrum not shown, lifetime 1.6 ms), which is a mixture of M (75%) and N (25%).

There are decreases in intensity around the overlapping discrete bands at 1693 and 1661 cm^{-1}, but these bands themselves seem to be retained at pH 10. No pH effect can be detected for an overlapping positive band at 1761 cm^{-1} due to Asp85. The pair of the bands at 1745 (–)/1738 (+) cm^{-1} in the spectrum at pH 7, which is due to the sum of the perturbations of Asp96 and Asp115, is similar to the feature that appeared in a previously reported spectrum (36), while the pair of bands at 1740 (+)/1732 (–) cm^{-1} at pH 10 is similar to that obtained for bacteriorhodopsin at pH 10 and 230 K (37). This difference could arise from a decrease in the perturbation of Asp96 in M at pH 10 (38).

The Broad Features in the Regions 2120-1780 cm^{-1} and 1725-1685 cm^{-1} Arise upon M Formation

Figure 3 shows changes in signal intensities at selected frequencies over the time course of the reaction up to 2 ms after the flash. In plots (b) through (d), the circles show the difference between the signal intensities at pH 7 and pH 10 averaged over the following spectral region: (b) between 1900 and 1800 cm^{-1} reflecting the broad feature, (c) between 1725 and 1685 cm^{-1}, and (d) between 1115 and 1035 cm^{-1}. These are compared with the time courses of M and N (circles and dots, respectively in Figure 3, a; details in the figure legend). The time course of M (multiplied by –1) is also superimposed on the plots of (b–d) as dots. The region below 1685 cm^{-1} is not examined because large discrete bands appear at 1661 cm^{-1} in the M-minus-BR spectrum and 1670 cm^{-1} in the N-minus-BR spectrum (5, 36). The region between 1800 and 1725 cm^{-1} is not relevant for the current work, because changes in this region are largely due to the perturbations of carboxylic acids. The region between 2120 and 2000 cm^{-1} was omitted because of high noise.

The alkaline-sensitive vibrational bands in the regions between 1900 and 1800 cm^{-1} (b), and between 1725 and 1685 cm^{-1} (c) arise almost concurrently with formation of M, and is preserved in N even after decay of M. In contrast, the time course of the broad band between 1115 and 1035 cm^{-1} (d) shows that this band arises in M and disappears with its decay.

Spectra of C_{15}-Deuterated Bacteriorhodopsin

The time-resolved data set (the average of 8 files) for C_{15}-deuterated bacteriorhodopsin was fitted with a 4-component model. For comparison, the corresponding data for unlabeled bacteriorhodopsin were also fitted with a 4-component model. Among the components from this fit, spectrum d_2 of unlabeled bacteriorhodopsin (lifetime 1.5 ms; thin line in Figure 1c) was coincident in shape with spectrum d_3 in the 6-component model, which was assigned to the M-minus-BR spectrum. The corresponding spectrum d_2 from C_{15}-deuterated bacteriorhodopsin (lifetime 1.8 ms) (thick line in Figure 1c) was used as the M-minus-BR spectrum for that sample. The 1168 cm^{-1} band was used as a ruler by which to gauge the amplitudes of both the labeled and unlabeled bacteriorhodopsin.

The 1761 cm^{-1} band due to Asp85 of M has the same amplitude in the spectra of both the labeled and unlabeled samples. Almost all other negative bands in the M-minus-BR spectrum of bacteriorhodopsin at pH 7 were affected by C_{15}-deuteration (Figure 1c). The changes caused by C_{15}-deuteration—the depletion of the 1200 cm^{-1} band, the shift of the trough at 1640 cm^{-1} to 1629 cm^{-1}, together with the unchanged 1168 cm^{-1} band—are completely coincident with the corresponding parts of a previously published time-resolved infrared spectrum covering a more limited frequency region (39). The negative bands at 1358, 1269, and 973 cm^{-1} are also consistent with those reported in the M-minus-BR spectrum of C_{15}-deuterated bacteriorhodopsin at 230 K (40). These arise in place of the bands at 1348 and 1252 cm^{-1} in unlabeled bacteriorhodopsin (Figure 1a) and are due to the vibrations of the Schiff base. Also, as shown in previous resonance Raman spectra of BR (41), the 1528 cm^{-1} band arising from the C=C stretching vibration is shifted to 1520 cm^{-1}.

This confirms that the spectrum of C_{15}-deuterated bacteriorhodopsin obtained in the present study is of sufficient quality and fidelity to be used in comparison with our earlier data from unlabeled bacteriorhodopsin to look for hitherto unidentified effects of C_{15}-deuteration on the spectrum.

The broad negative band between 1115 and 1035 cm^{-1} in the M-minus-BR spectrum of unlabeled bacteriorhodopsin, which disappeared in the spectrum at pH 10, also disappears in the M-minus-BR spectrum of C_{15}-deuterated bacteriorhodopsin (Figure 1c). Previous papers (41–43) have suggested that the C—C and C—N stretching vibrations of the side chain of Lys216 contribute to vibration bands in the 1150-1030 cm^{-1} region. The present results also suggest that these vibrational bands are further coupled with the retinal C_{15}—H bending vibrations.

The spectrum of C_{15}-deuterated enzyme in the region between 2120 and 1780 cm^{-1} (thick line in Figure 4) is nearly coincident with the spectrum of the unlabeled sample (thin line). The C_{15}-D trace has more noise, but the trace from unlabeled enzyme tracks the center of the noise envelope of the C_{15}-D trace. To confirm that no significant difference is concealed by this noise, the two spectra were further compared with the M-minus-BR spectrum at pH 10 (spectral component d_2 from the 4-exponential fit; dotted line), where there is clearly less negative intensity in this region than in the pH 7 spectrum (see also Figure 2). From 2120 to 2000 cm^{-1}, the pH 10 trace (dotted line) is not clearly distinguishable from the center of the C_{15}-D bacteriorhodopsin trace (solid line), but beginning around 2000 cm^{-1}, as the frequency decreases, one can see that the spectrum of C_{15}-D enzyme gradually deviates below the spectrum at pH 10, until by 1780 cm^{-1} the pH 10 trace is clearly no longer at the center of the C_{15}-D trace noise envelope, and essentially outside that envelope. This indicates that the negative broad feature, obtained by subtracting the spectrum at pH 10 from that at pH 7, is insensitive to C_{15}-deuteration in the region above 1780 cm^{-1}. In contrast, the negative feature at pH 7 (thin line) in the region between 1725 and 1685 cm^{-1} is clearly depleted by C_{15}-deuteration (thick line).

Effect of pH 10 on the Water Vibration at 3657 cm^{-1} in M

Positive bands at 3671 and 3657 cm^{-1}, and a negative band at 3645 cm^{-1}, which are present in spectrum d_3, the pure M-minus-BR spectrum at pH 7 (dotted line in Figure 5, a), have been previously assigned to water O—H stretching vibrations (5). The effect on these bands of increasing the pH to 10 can be seen by comparison with spectrum d_3, which is the pure M-minus-BR spectrum at pH 10 (solid line in Figure 5, a).

The 3645 cm^{-1} band of BR is seen as a trough in the spectra at pH 10, as it is at pH 7. The 3671 and 3657 cm^{-1} bands arise from water molecules that lose hydrogen bonding upon M formation. The 3671 cm^{-1} band, which is observed in M at pH 7 (dotted line in a), remains visible at pH 10 (solid line in a). The same band was observed in the M intermediate of bacteriorhodopsin when the photoreaction was carried out at 230 K (27, 44). This band was considerably diminished in intensity in the F219L mutant (44). Hence, this band is due to a water molecule in the neighborhood of Phe219 close to Asp96 on the cytoplasmic side (5). The other positive band, at 3657 cm^{-1}, which is observed in the spectrum at pH 7 (dotted line in a), loses intensity at pH 10 (solid line in a), suggesting that it arises from a water molecule perturbed by deprotonation of PRG. In the previous low temperature study, the 3657 cm^{-1} band was abolished in two different mutants of Arg82: R82A and R82K (45). The frequency of this vibration corresponds to a water O—H bond free from hydrogen bonding, suggesting that M formation is accompanied by liberation of a water molecule from Arg82.

In spectra d_4 and d_5 at pH 10, the 1670 cm^{-1} band of BR, characteristic of the N-minus-BR spectrum, appears, and the intensity in the higher frequency part of the band of Asp85 around 1761 cm^{-1} is decreased (not shown). This part of the vibration due to Asp85 in M, together with the 1661 cm^{-1} band of M, could be completely removed from spectra d_4 and d_5 by the subtraction of spectrum d_3, multiplied by factors of 0.75 and 0.3 (the contributions of M), respectively. Thus, the content of M in d_4 (b) and d_5 (c) at pH 10 can be estimated at 75%, and 30%, respectively. These values allow the pH 10 spectra (solid lines) to be compared with the corresponding spectra at pH 7 (dotted lines), which include contributions of 60% and 45% of M for d_4 and d_5 (5), respectively. The remaining part of the spectra is mainly due to N, but a small fraction (8%) of O is present in d_5 at pH 7. Even as M is replaced by N in this series of spectra at pH 7 (dotted lines in b and c), the intensity of the band at 3657 cm^{-1} at pH 7 is retained, in contrast to the diminishing 3671 cm^{-1} band. The 3657 cm^{-1} band loses intensity at pH 10, whereas the band at 3671 cm^{-1} is preserved (solid lines vs. dotted lines). Thus, the 3657 cm^{-1} band is due to a water molecule liberated from Arg82 and appears throughout M and N, intermediates in which the PRG is deprotonated.

DISCUSSION

Spectral Changes Caused by Deprotonation of the PRG

We examined the effect of deprotonation of the PRG on the M-minus-BR spectrum by using the M-minus-BR spectrum of bacteriorhodopsin at pH 10 as a baseline (Figure 1, b). The difference between these two spectra, which reflects deprotonation of the PRG, has negative intensity spreading out broadly over a range from 2120 cm^{-1} to around 1655 cm^{-1} (Figure 2). Overlapping discrete bands at 1761, 1693 and 1661 cm^{-1} are conserved at pH 10. The remaining difference above 1685 cm^{-1} is an unstructured negative vibrational band. Below, we will discuss two parts of this band, the region above 1780 cm^{-1}, that is insensitive to C_{15}-deuteration, and the region between 1725 and 1685 cm^{-1}, that is sensitive to C_{15}-deuteration (Figure 4). All these changes arise concurrently with M formation and persist even after M decay (Figure 3, b, c), indicating that these bands lose intensity in M upon deprotonation of the PRG. Another broad band between 1115 and 1035 cm^{-1} is also abolished at pH 10 (Figure 1, b) and upon C_{15}-deuteration (Figure 1, c). This band is depleted in M, but is restored in N (Figure 3, d), indicating a correlation with the protonation state of the Schiff base as well as that of the PRG.

Loss of Delocalized Proton in PRG

The broad band of BR in the region above 1800 cm^{-1}, that is eliminated in the L-to-M transition, was earlier described by Rammelsberg et al (25). A convex feature around 2000 cm^{-1} was later revealed to be a non-specific heating effect, since it could be reproduced by elevating the temperature of a bacteriorhodopsin sample by 0.2°C, and also by laser excitation of a dye sample (26). In our study the heating effect could be monitored by a comparison with the spectrum at pH 10. The downward deviation of the spectrum at pH 7 compared to the spectrum at pH 10 (Figure 2) is due to the signal associated with the deprotonation of the PRG.

This unstructured negative band in the region above 1780 cm^{-1} is sensitive to ^2H_2O substitution (46). Most likely this is a continuum band that arises from proton polarizability ascribed to protons delocalized between hydrogen-bonding groups (46, 47). Mutations that replace the residues Glu204, Glu194 and Tyr83, which surround the water molecules in the PRG, severely affect the intensity of the negative band between 1900 and 1800 cm^{-1} (14). Thus, the broad band in the region between 2120 and 1780 cm^{-1} can be regarded as a continuum band due to proton delocalization in the hydrogen bonding network composed of

water molecules, as well as Glu204, Glu194 and Tyr83, as proposed earlier (14). Abolition of the continuum band in M could be due to the loss of a proton from this network.

Connection of Tyr57 and Asp212 with Arg82 and its Disruption in M

The previous studies have shown very rapid formation of M in the mutant R82A (15, 48) and also in Y57F (17), suggesting that M formation is associated with liberation of Arg82 and Tyr57 from their interactions. This is in accordance with the fact that the continuum band appears earlier in the R82Q and Y57F mutants than in wild type (14). A visible spectroscopic study has revealed that the R82A mutation diminishes the effect of ^2H_2O substitution on the rate of M formation, indicating the operation of a cooperative rearrangement of hydrogen bonding involving Arg82, upon M formation (49). The current study further suggests that a water molecule that forms a hydrogen bond to Arg82 is liberated upon deprotonation of PRG. The structure in Figure 6, which is based on crystallographic models of BR (18), shows that Tyr57 interacts with Water407, and Asp212 with Water 406. These water molecules interact further with one of the guanidium nitrogen atoms of Arg82. The interaction is lost when the guanidium group of Arg82 changes orientation toward Glu194 in M (50).

Interaction of the Carbonyl Groups in Helix G with the Schiff

The unstructured band in the region between 1725 and 1685 cm^{-1} may be derived from backbone carbonyl groups. A previous study (51) has shown, though this was not explicitly described by the authors, that negative intensity around 1693 cm^{-1} in the M-minus-BR spectrum diminishes in the spectrum of 1-[^{13}C-Lys]-labeled bacteriorhodopsin. This may reflect breaking of hydrogen bonding between the backbone carbonyl group of Lys216 and the backbone amide of Gly220, as observed in the crystallographic structure of M (52, 53).

The effect of C_{15}-deuteration on these vibrations could also arise from interaction with the Schiff base. The protonated Schiff base confers a positive charge on the chromophore, strengthening the dipole in the C_{15}—H bond of the Schiff base. The coupled vibrations of the backbone carbonyl groups that appear in the 1725-1685 cm^{-1} region may arise by acquiring larger infrared intensities, and frequency shifts, probably toward higher frequency, through transition dipole coupling (54) with the C_{15}—H in-plane bending vibrations due to the Schiff base at 1348 and 1252 cm^{-1} (Figure 1c). The broad band loses intensity upon C_{15}-deuteration (Figure 4) because little or no coupling occurs to the C_{15}—^{2}H bending vibrations, since it has a much lower frequency, 973 cm^{-1} (Figure 1, c). The backbone carbonyl group of Asp212, which is the nearest group to C_{15}—H (Figure 6), may be one of the perturbed backbone groups involved in the vibrations in the 1725-1685 cm^{-1} region. Loss of this intensity in M could be at least partly due to loss of the interaction of the Schiff base with the backbone carbonyl of Asp212. However, accounting for persistent loss in N, where the Schiff base is reprotonated, is not straightforward. Differences in the structure around the Schiff base in N or other changes in interaction such as described below must be taken into considerations.

Connection of Tyr57 with Helix G and its Disruption in M

Liu et al. (55) have shown that the unstructured band in the region around 1705 cm^{-1} is depleted in [ring ^{2}H$_4$]-Tyr57 bacteriorhodopsin, though they did not make note of it. The ring C—H itself is not responsible for the vibrations around 1705 cm^{-1} (56). This vibration frequency is most likely due to a backbone carbonyl group. The crystallographic models of BR in Figure 6 (18) show that the backbone carbonyl oxygen atom of Phe208 is located close to the phenolic oxygen atom of Tyr57, suggesting coupling of the vibration of Tyr57 to a backbone carbonyl vibration, most likely to that of Phe208.

The phenolic oxygen atom of Tyr57 also interacts with one of the carboxyl oxygen atoms of Asp212. Oxygen atoms of Tyr57, Asp212, Phe208 together with two water molecules form a cluster close to the guanidium-group of Arg82. The backbone carbonyl groups of Glu204, Phe208, Asp212 and Lys216 also lie on a straight line in helix G, in the crystallographic structure of BR, and may contribute to the broad band between 1725 and 1685 cm^{-1} together with Tyr57 and C_{15}—H.

No perturbation of Tyr57 itself has been detected upon M formation of wild type (55). Nevertheless, in Y57D the deprotonation of Asp57 occurs in place of deprotonation of the Schiff base (57). The deprotonation in M of wild type may also occur from the neighborhood of Tyr57, or the site interacting with Tyr57. This site may be an important site to stabilize M. Circumstantial evidence that is worth noting here is that the V210Y/P200T mutant of bacteriorhodopsin can interact with the transducer protein of sensory rhodopsin II, HtrII, and form a very stable M intermediate (58). Val210 is a residue opposite to Phe208 and Asp212 with respect to the helix axis (below Phe208 in Figure 6).

Liberation of the Carboxyl Group of Asp212 from Constraints of Arg82 and Helix G

The continuum band in the region between 2120 and 1780 cm^{-1} is due to the delocalized proton in the PRG. The broad band in the region between 1725 and 1685 cm^{-1} is due to the backbone carbonyl groups of helix G coupled with Tyr57 and C_{15}—H of the Schiff base. Both are present in BR, but absent at pH 10 with the deprotonation of the PRG, and are depleted in M and do not recover in N (Figure 3). The water band at 3657 cm^{-1}, that appears concurrently, results from the disconnection of water molecules hydrating Asp212 from Arg82. These events may lead to the disconnection of the Tyr57-Asp212 pair from Arg82 and the C=O of Phe208 together with the disconnection of C_{15}-H from the C=O of Asp212. As a result, Asp212 becomes free from the constraints exerted by Arg82, and helix G and is able to interact with Asp85 through water molecules (see review 4). The protonated form of Asp85 would be stabilized in this way.

Acknowledgments

Abbreviations

PRG   Proton-release group

BR   initial unphotolyzed state of bacteriorhodopsin with all-trans retinal chromophore

References

1. Lozier RH, Bogomolni RA, Stoeckenius W. Bacteriorhodopsin: A light-driven proton pump in *Halobacterium halobium*. Biophys J. 1975; 15:955–963. [PubMed: 1182271]

2. Xie A, Nagle JF, Lozier RH. Flash spectroscopy of purple membrane. Biophys J. 1987; 51:627–635. [PubMed: 3580488]

3. Maeda A, Morgan JE, Gennis RB, Ebrey TG. Water as a cofactor in the unidirectional light-driven proton transfer steps in bacteriorhodopsin. Photochem Photobiol. 2006; 82:1396–1405.

4. Morgan JE, Gennis RB, Maeda A. A role for internal water molecules in proton affinity changes of the Schiff base and Asp85 for one-way proton transfer in bacteriorhodopsin. Photochem Photobiol. 2008; 84:1038–1045. [PubMed: 18557823]

5. Morgan JE, Vakkasoglu AS, Gennis RB, Maeda A. Water structural changes in the L and M intermediates of bacteriorhodopsin as revealed by time-resolved step-scan FTIR spectroscopy. Biochemistry. 2007; 46:2787–2796. [PubMed: 17300175]

6. Lórenz-Fonfría VA, Furutani Y, Kandori H. Active internal waters in the bacteriorhodopsin photocycle. A comparative study of the L and M intermediates at room and cryogenic temperatures by infrared spectroscopy. Biochemistry. 2008; 47:4071–4081. [PubMed: 18321068]

7. Váró G, Keszthelyi L. Photoelectric signals from dried oriented purple membranes of *Halobacterium halobium*. Biophys J. 1983; 43:47–51. [PubMed: 6309264]

8. Váró G, Lanyi JK. Distortion in the photocycle of bacteriorhodopsin at moderate dehydration. Biophys J. 1991; 59:313–322. [PubMed: 2009355]

9. Heberle J, Dencher NA. Surface-bound optical probes monitor proton translocation and surface potential changes during the bacteriorhodpsin photocycle. Proc Natl Acad Sci USA. 1992; 89:5996–6000. [PubMed: 1497755]

10. Zimanyi L, Váró G, Chang M, Ni B, Needleman R, Lanyi JK. Pathways of proton release in the bacteriorhodopsin photocycle. Biochemistry. 1992; 31:8535–8543. [PubMed: 1327104]

11. Brown LS, Sasaki J, Kandori H, Maeda A, Needleman R, Lanyi JK. Glutamic acid 204 in the terminal proton release group at the extracellular surface of bacteriorhodopsin. J Biol Chem. 1995; 270:27122–27126. [PubMed: 7592966]

12. Balashov SP, Imasheva ES, Ebrey TG, Chen N, Menick DR, Crouch RK. Glutamate-194 to cysteine mutation inhibits fast light-induced proton release in bacteriorhodopsin. Biochemistry. 1997; 36:8671–8676. [PubMed: 9289012]

13. Dioumaev AK, Richter H-T, Brown LS, Tanio M, Tuzi S, Saitô H, Kimura Y, Needleman R, Lanyi JK. Existence of a proton transfer chain in bacteriorhodopsin: Participation of Glu-194 in the release of protons to the extracellular surface. Biochemistry. 1998; 37:2496–2506. [PubMed: 9485398]

14. Garczarek F, Brown LS, Lanyi JK, Gerwert K. Proton binding within a membrane protein by a protonated water cluster. Proc Natl Acad Sci USA. 2005; 102:3633–3638. [PubMed: 15738416]

15. Balashov SP, Govindjee R, Kono M, Imasheva ES, Lukashev E, Ebrey TG, Crouch RK, Menick DR, Feng Y. Effect of the arginine-82 to alanine mutation in bacteriorhodopsinon dark adaptation, proton release, and the photochemical cycle. Biochemistry. 1993; 32:10331–10343. [PubMed: 8399176]

16. Govindjee R, Misra S, Balashov S, Ebrey T, Crouch RK, Menick DR. Arginine-82 regulates the pK_a of the group responsible for the light-driven proton release in bacteriorhodopsin. Biophys J. 1996; 71:1011–1023. [PubMed: 8842238]

17. Govindjee R, Kono M, Balashov SP, Imasheva E, Sheves M, Ebrey TG. Effect of substitution of tyrosine 57 with asparagine and phenylalanine on the properties of bacteriorhodopsin. Biochemistry. 1995; 34:4828–4838. [PubMed: 7718589]

18. Luecke H, Schobert B, Richter HT, Cartailler JP, Lanyi JK. Structure of bacteriorhodopsin at 1.55 Å resolution. J Mol Biol. 1999; 291:899–911. [PubMed: 10452895]

19. Belrhali H, Nollert P, Royant A, Menzel C, Rosenbusch JP, Landau EM, Pebay-Peyroula E. Protein, lipid and water organization in bacteriorhodopsin crystals: a moleculear view of the purple membrane at 1.9 Å resolution. Structure. 1999; 7:909–917. [PubMed: 10467143]

20. Spaasov VZ, Luecke H, Gerwert K, Bashford D. pK_a calculations suggest storage of an excess proton in a hydrogen-bonded water network in bacteriorhodopsin. J Mol Biol. 2001; 312:203–219. [PubMed: 11545597]

21. Mathias G, Marx D. Structures and spectral signatures of protonated water networks in bacteriorhodopsin. Proc Natl Acad Sci USA. 2007; 104:6980–6985. [PubMed: 17438299]

22. Richter H-T, Brown LS, Needleman R, Lanyi JK. A linkage of the pK_a's of asp-85 and glu204 forms part of the reprotonation switch of bacteriorhodopsin. Biochemistry. 1996; 35:4054–4062. [PubMed: 8672439]

23. Balashov SP, Imasheva ES, Givindjee R, Ebrey TG. Titration of aspartate-85 in bacteriorhodopsin: What it says about chromophore isomerization and proton release. Biophys J. 1996; 70:473–481. [PubMed: 8770224]

24. Váró G, Lanyi JK. Kinetics and spectroscopic evidence for an irreversible step between deprotonation and reprotonation of the Schiff base in the baterorhodopsi photocycle. Biochemistry. 1991; 30:5008–5015. [PubMed: 1645187]

25. Rammelsberg R, Huhn G, Lübben M, Gerwert K. Bacteriorhodopsin's intramolecular proton-release pathway consists of a hydrogen-bonded network. Biochemistry. 1998; 37:5001–5009. [PubMed: 9538019]

26. Garczarek F, Wang J, El-Sayed MA, Gerwert K. The assignment of the different infrared continuum absorbance changes observed in the 3000–1800 cm^{-1} region during the bacteriorhodopsin photocycle. Biophys J. 2004; 87:2676–2682. [PubMed: 15298873]

27. Garczarek F, Gerwert K. Functional waters in intraprotein proton transfer monitored by FTIR difference spectroscopy. Nature. 2006; 439:109–112. [PubMed: 16280982]

28. Balashov SP, Govindjee R, Ebrey T. Red shift of the purple membrane absorption band and the deprotonation of tyrosine residues at high pH. Biophys J. 1991; 60:475–490. [PubMed: 19431801]

29. Maeda A, Balashov SP, Lugtenburg J, Verhoeven M, Herzfeld J, Belenky M, Gennis RB, Tomson FL, Ebrey TG. Interaction of internal water molecules with the Schiff base in the L intermediate of the bacteriorhodopsin photocycle. Biochemistry. 2002; 41:3803–3809. [PubMed: 11888299]

30. Provencher, SW.; Vogel, RH. Regularization techniques for inverse problems in molecular biology: in Numerical Treatment of Inverse Problems in Differential and Integral Equations. Deuflhard, P.; Hairer, E., editors. Vol. 1983. Birkhäuser; Boston: 1983. p. 304-319.

31. Chizhov I, Chenavskii DS, Engelhard M, Mueller KH, Zubov BV, Hess B. Spectrally silent transitions in the bacteriorhodopsin photocycle. Biophys J. 1996; 71:2329–2345. [PubMed: 8913574]

32. Szundi I, Lewis JW, Kliger DS. Deriving reaction mechanism from kinetic spectroscopy. Application to late rhodopsin intermediates. Biophys J. 1997; 73:688–702. [PubMed: 9251787]

33. Braiman MS, Dioumaev AK, Lewis JR. A large photolysis-induced pK_a increase of the chromophore counterion in bacteriorhodopsin: Implications for ion transport mechanisms of retinal proteins. Biophys J. 1996; 70:939–947. [PubMed: 8789111]

34. Rödig C, Chizhov I, Weidlich O, Siebert F. Time-resolved step-scan Fourier transform infrared spectroscopy reveals differences between early and late M intermediates of bacteriorhodopsin. Biophys J. 1999; 76:2687–2701. [PubMed: 10233083]

35. Zscherp C, Schlessinger R, Tittor J, Oesterhelt D, Heberle J. In situ determination of transient pK_a changes of internal amino acids of bacteriorhodopsin by using time-resolved attenuated total reflection Fourier transform infrared spectroscopy. Proc Natl Acad Sci USA. 1999; 96:5498–5503. [PubMed: 10318912]

36. Hessling B, Souvinir G, Gerwert K. A model-independent approach to assigning bacteriorhodopsin's intramolecular reactions to photocycle intermediates. Biophys J. 1993; 65:1929–1941. [PubMed: 8298022]

37. Sasaki J, Lanyi JK, Needleman R, Yoshizawa T, Maeda A. Complete identification of C=O stretching vibrational bands of protonated aspartic acid residues in the difference infrared spectra of M and N intermediates of bacteriorhodopsin. Biochemistry. 1994; 33:3178–3184. [PubMed: 8136352]

38. Maeda A, Tomson FL, Gennis RB, Kandori H, Ebrey TG, Balashov SP. Relocation of internal bound water in bacteriorhodopsin during the photoreaction of M at low temperature: an FTIR study. Biochemistry. 2000; 39:10154–10162. [PubMed: 10956004]

39. Siebert F, Mäntele W. Investigation of the primary photochemistry of bacteriorhodopsin by low temperature Fourier-transform infrared spectroscopy. Eur J Biochem. 1983; 130:565–573. [PubMed: 6825710]

40. Maeda A, Sasaki J, Pfefferlé JM, Shichida Y, Yoshizawa T. Fourier transform infrared spectral studies on the Schiff base mode of all-trans bacteriorhodopsin and its photointermediates, K and L. Photochem Photobiol. 1991; 54:911–921.

41. Smith SO, Braiman MS, Myers AB, Pardoen JA, Courtin JML, Winkel C, Lugtenburg J, Mathies RA. Virational analysis of the *all-trans*-retinal chromophore in light-adapted bacteriorhodopsin. J Am Chem Soc. 1987; 109:3108–3125.

42. McMaster E, Lewis A. Evidence for light-induced lysine conformational changes during the primary event of the bacteriorhodopsin photocycle. Biochem Biophys Res Comm. 1988; 156:86–91. [PubMed: 3140817]

43. Gat Y, Grossjean M, Pinevsky I, Takei H, Rothman Z, Sigrist H, Lewis A, Sheves M. Participation of bacteriorhodopsin active-site lysine backbone in vibrations associated with retinal photochemistry. Proc Natl Acad Sci USA. 1992; 89:2434–2438. [PubMed: 1549607]

44. Yamazaki Y, Kandori H, Needleman R, Lanyi JK, Maeda A. Interaction of the protonated Schiff base with the peptide backbone of valine 49 and the intervening water molecule in the N photointermediate of bacteriorhodopsin. Biochemistry. 1998; 37:1559–1564. [PubMed: 9484226]

45. Hatanaka M, Sasaki J, Kandori H, Ebrey TG, Needleman R, Lanyi JK, Maeda A. Effects of arginine-82 on the interactions of internal water molecules in bacteriorhodopsin. Biochemistry. 1995; 35:6308–6312. [PubMed: 8639574]

46. Wang J, El-Sayed MA. Proton polarizability of hydrogen-bonded network and its role in proton transfer in bacteriorhodopsin. J Phys Chem A. 2000; 104:4333–4337.

47. Zundel G. Hydrogen bonds with large proton polarizability and proton transfer processes in electrochemistry and biology. Adv Chem Phys. 2000; 111:1–217.

48. Balashov SP, Govindjee R, Imasheva ES, Misra S, Ebrey TG, Feng Y, Crouch RK, Menick DR. The two pK_a's of aspartate-85 and control of thermal isomerization and proton release in the arginine-82 to lysine mutant of bacteriorhodopsin. Biochemistry. 1995; 34:8820–8834. [PubMed: 7612623]

49. Brown LS, Needleman R, Lanyi JK. Origins of deuterium kinetic isotope effects on the proton transfers of the bacteriorhodopsin photocycle. Biochemistry. 2000; 39:938–945. [PubMed: 10653637]

50. Luecke H, Schobert B, Richter H-T, Cartailler J-P, Lanyi JK. Structural changes in bacteriorhodopsin during ion transport at 2 angstrom resolution. Science. 1999; 286:255–260. [PubMed: 10514362]

51. Takei H, Gat Y, Rothman Z, Lewis A, Sheves M. Active site lysine backbone undergoes conformational changes in the bacteriorhodopsin photocycle. J Biol Chem. 1994; 269:7387–7389. [PubMed: 8125956]

52. Luecke H, Schobert B, Cartailler JP, Richter HT, Rosengarth A, Needleman R, Lanyi JK. Coupling photoisomerization of retinal to directional transport in bacteriorhodopsin. J Mol Biol. 2000; 300:1237–1255. [PubMed: 10903866]

53. Takeda K, Matsui Y, Kamiya N, Adachi S, Okumura H, Kouyama T. Crystal structure of the M intermediate of bacteriorhodopsin: Allosteric structural changes mediated by sliding movement of a transmembrane helix. J Mol Biol. 2004; 341:1023–1037. [PubMed: 15328615]

54. Barth A, Zscherp C. What vibrations tell us about proteins. Quart Rev Biophys. 2002; 35:369–430.

55. Liu X-M, Sonar S, Lee C-P, Coleman M, RajBhandary UL, Rothschild KJ. Site-directed isotope labeling and FTIR spectroscopy: assignment of tyrosine bands in the bR → M difference spectrum of bacteriorhodopsin. Biophys Chem. 1995; 56:63–70. [PubMed: 7662870]

56. Rothschild KJ, Roepe P, Ahl PL, Earnest TN, Bogomolni RA, Das Gupta SK, Mulliken CM, Herzfeld J. Evidence for a tyrosine protonation change during the primary phototransition of bacteriorhodopsin at low temperature. Proc Natl Acad Sci USA. 1986; 83:347–351. [PubMed: 3001733]

57. Sonar S, Marti T, Rath P, Fischer W, Coleman M, Nilsson A, Khorana HG, Rothschild KJ. A predicted proton pathway in the bacteriorhodopsin mutant Tyr57→ Asp. J Biol Chem. 1994; 269:28851–28858. [PubMed: 7961844]

58. Sudo Y, Spudich JL. Three strategically placed hydrogen-bonding residues convert a proton pump into sensory receptor. Proc Natl Acad Sci USA. 2006; 103:116129–16134.

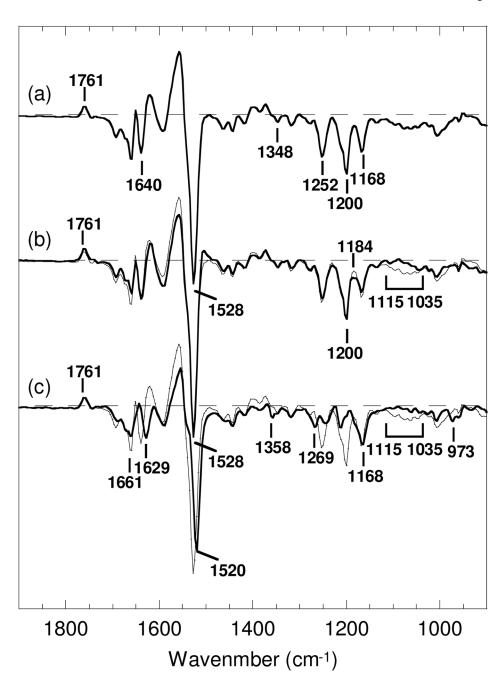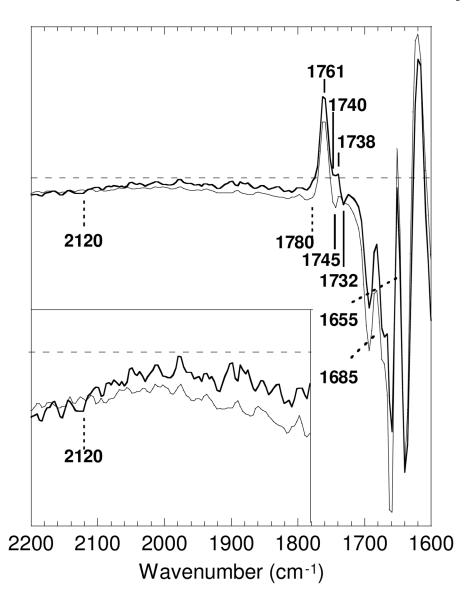59. DeLano, W. PYMOL. DeLano Scientific; San Carlos, CA: 2002.

Figure 1.
M-minus-BR spectra of: unlabeled bacteriorhodopsin at (a) pH 7, (b) pH 10 and (c) C_{15}-deuterated bacteriorhodopsin at pH 7. The spectrum of (a) is duplicated with thin lines in (b) and (c). The full length of the ordinate corresponds to 0.020 absorbance unit for the spectra of unlabeled bacteriorhodopsin at pH 7, 0.010 for the spectrum at pH 10 (b), and 0.009 for the spectrum of C_{15}-D bacteriorhodopsin at pH 7 (c).

Figure 2.
Comparison of the M-minus-BR spectrum at pH 10 (thick lines) to that at pH 7 (thin lines) by expanding the region of the spectra between 2200 and 1600 cm^{-1}. The full length of the ordinate corresponds to 0.0023 absorbance unit for the spectrum of unlabeled bacteriorhodopsin at pH 7, and 0.00115 absorbance unit for the spectrum of unlabeled bacteriorhodopsin at pH 10. The ordinate of the spectra in the inset was expanded 4 fold.
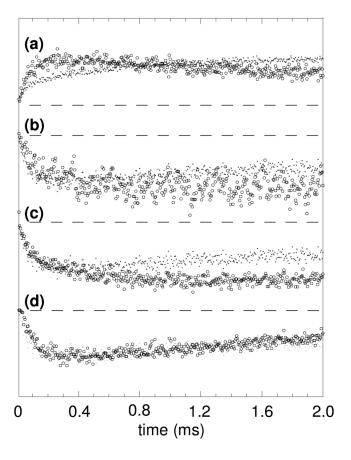
Figure 3.
Time courses of the bleaching of the pH 10-sensitive bands in comparison with formation of M after the flash. Red traces in (b) through (d) were obtained by subtracting the plots at pH 10 that were multiplied by the factor 2.0 to adjust amplitudes to match those at pH 7. (a) Time course for M (circles); the average of the intensities between 1780 and 1765 cm^{-1} where the contribution of the 1761 cm^{-1} band of M dominates that of the 1757 cm^{-1} band of N was calculated and then the average of the intensities between 1790 and 1780 cm^{-1} was subtracted as the baseline. Time course for N (dots); The average of the intensities between 1755 and 1750 cm^{-1} where the contribution of the 1757 cm^{-1} band of N dominates that of the 1761 cm^{-1} band of M was calculated and then the average of the intensities between 1790 and 1780 cm^{-1} was subtracted as the baseline. (b) The average of the intensities in the region between 1900 and 1800 cm^{-1}. (c) The average of the intensities in the region between 1725 and 1685 cm^{-1}. (d) The average of intensities between 1115 and 1035 cm^{-1}. The results of (b), (c), and (d) were plotted by multiplying by 2.2, 0.44 and 0.37, respectively, (circles) to allow visual comparison with the time course for M formation (the superimposing dots) which was obtained from the plots in (a) by multiplying by −1. Broken lines show the zero in the difference absorbance.
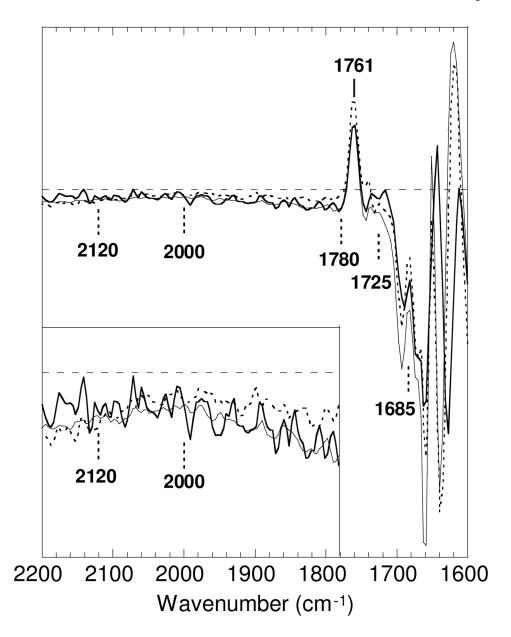
Figure 4.
Comparison of the M-minus-BR spectrum of C_{15}-deuterated bacteriorhodopsin at pH 7 (thick lines) to that of unlabeled bacteriorhodopsin at pH 7 in H_2O (thin lines) by expanding the region of the spectra between 2200 and 1600 cm^{-1}. The spectrum at pH 10 is included as a dotted line. The full length of the ordinate corresponds to 0.0023 absorbance unit for the spectrum of unlabeled bacteriorhodopsin at pH 7, 0.00115 absorbance unit for pH 10 and 0.00104 absorbance unit for the spectrum of C_{15}-D bacteriorhodopsin at pH 7. The spectra of unlabeled bacteriorhodopsin at pH 7 and pH 10 obtained as d_2 component spectra from 4-exponential fits are almost identical but not coincident in noise with those in Figure 2 obtained as d_3 component spectra from 6-exponential fits. The ordinate of the spectra in the inset was expanded 4 fold.
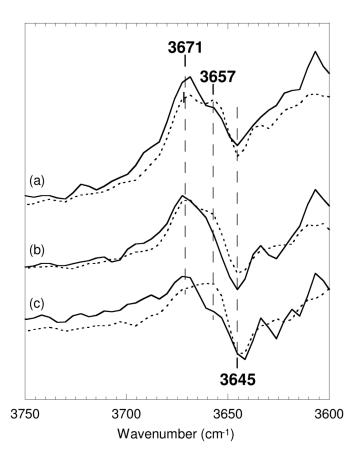
Figure 5.
Comparison of the water O—H stretching vibrational bands of bacteriorhodopsin at pH 10 (solid lines) to those at pH 7 (dotted lines) in the kinetic intermediate spectra d_3 (a), d_4 (b), and d_5 (c); see Materials and Methods. The full length of the ordinate corresponds to 0.0012 absorbance unit for unlabeled bacteriorhodopsin at pH 7, and to 0.0006 absorbance unit for unlabeled bacteriorhodopsin at pH 10.
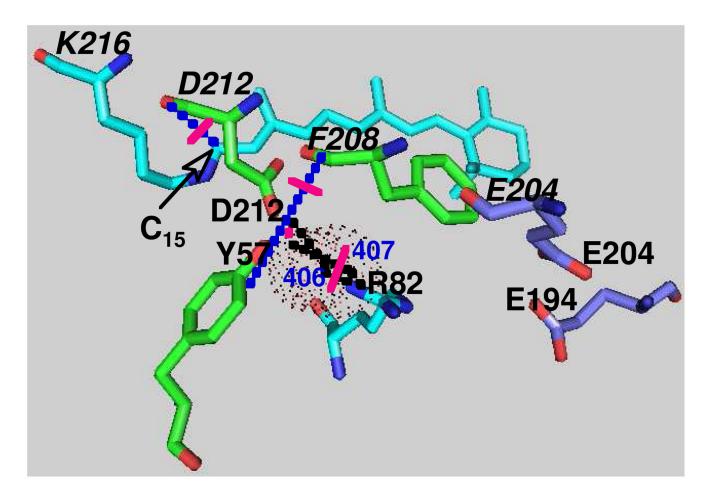
Figure 6.
Structure of bacteriorhodopsin in the unphotolyzed state (BR) on the basis of the protein
databank entry 1c3w (18), showing the locations of the side-chains (with plain letters), the
backbone carbonyls (with italic letters) and water molecules (with numbers in blue letters)
that are discussed in the text. Water molecules are shown as dotted spheres. Dotted lines
show the interaction in BR (black for hydrogen bonding, blue for dipole interactions).
Strikethroughs in red show the interruption of the interaction that occurs in M. Molecular
graphic representations were generated with PYMOL (59).